The Development of a Control System for a 5 Kilowatt Free Piston Stirling Engine Convertor

Raymond L. Kirby and Nick. Vitale

Abstract. **The new NASA Vision for Exploration, announced by President Bush in January 2004, proposes an ambitious program that plans to return astronauts to the moon by the 2018 time frame. A recent NASA study entitled "Affordable Fission Surface Power Study" recommended a 40 kWe, 900 K, NaK-cooled, Stirling convertors for 2020 launch. Use of two of the nominal 5 kW convertors allows the system to be dynamically balanced. A group of four dual-convertor combinations that would yield 40 kWe can be tested to validate the viability of Stirling technology for space fission surface power systems.**

The work described in this paper deals specifically with the control system for the 5 kW convertor described in the preceding paragraph. This control system is responsible for maintaining piston stroke to a setpoint in the presence of various disturbances including electrical load variations. Pulse starting of the Free Piston Stirling Engine (FPSE) convertor is also an inherent part of such a control system. Finally, the ability to throttle the engine to match the required output power is discussed in terms of setpoint control. Several novel ideas have been incorporated into the piston stroke control strategy that will engender a stable response to disturbances in the presence of midpoint drift while providing useful data regarding the position of both the power piston and displacer.

***Index Terms*—Free piston Stirling engine, stroke control.**

INTODUCTION

Kankam [4] et al. have investigated the dynamic properties of the Free-Piston Stirling Engine (FPSE). The FPSE stroke amplitude is a function of electrical load. As the load resistance is decreased the stroke amplitude will be lowered to a new stable equilibrium point or stall if the resistance is too small to maintain oscillation. As the load resistance is increased the stroke amplitude will increase to a new equilibrium point or hit the mechanical limits. Modeling the dynamic behavior of the FPSE in response to load resistance changes is the focus of this work.

The FPSE used in this work will be capable of producing 400 volts RMS at 5 kilowatts with a 22 mm peak-to-peak stroke at a frequency of 85 hertz. The engine will be started by applying a short AC burst at 85 hertz. Once the engine stroke is sustained the stroke control circuit will maintain the stroke amplitude at the setpoint value. The setpoint range is between 11 and 22 mm peak to peak.

A master controller will monitor all subordinate controllers including: the stroke controller, the hot oil controller, and the cooling loop. The stroke controller is responsible for maintaining the FPSE convertor piston stroke at the desired setpoint. The hot oil controller is responsible for delivering the hot oil that is used to provide heat to the hot end of the FPSE convertor and keep it at the desired temperature. The cooling loop controller is responsible for keeping the cold end of the FPSE convertor at a desired temperature. In the event there is a problem with any of these subordinate controllers the master controller will implement a safe shutdown of the entire system. A touch screen will provide the user interface for the control system. Process data will be displayed and operator functions can be performed via the touch screen. For example, the stroke setpoint can be changed via the touch screen.

The objective of this work was to understand the dynamic characteristics of a free piston Stirling engine and to establish an acceptable method of controlling the piston stroke of the engine. In order to experiment with various control strategies, without damage to the actual engine, a dynamic model of the engine was developed. Initially a linear model is used and later extended to a non-linear model. The non-linear model was then used to analyze different control strategies. Once a control strategy was selected the implementation of the control strategy is discussed. The dynamic model is shown in Figure 1.

I. THE FPSE DYNAMIC MODEL

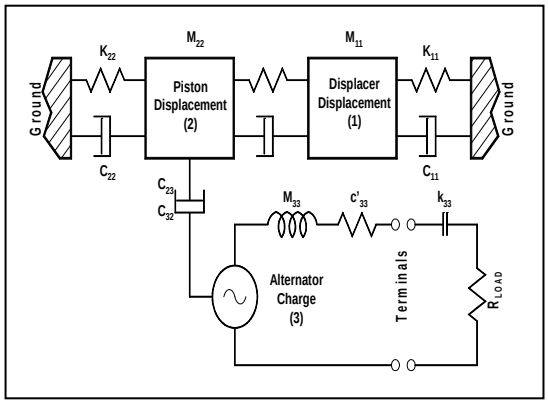

Figure 1: Elements of the FPSE Model

The convertor is mounted on a heavy steel plate that is sized so that the vibration amplitude of the convertor casing is limited to approximately 0.001" (25 μm). The engine casing can be considered as ground as shown in Figure 1. The

relative spring and damping parameters: K_{12}, K_{21}, C_{12}, and C_{21} represent the engine thermodynamics and are determined from the HFAST2 thermodynamics code. Due to the temperature difference between the expansion and compression spaces the two spring coefficients and the two damping coefficients are not equal to each other as would normally be the case in a passive dynamic system. The difference between the spring coefficients gives the dynamic system the ability to generate power. The hot end temperature is maintained at 650 ^{0}K while the cold end is 325 ^{0}K.

The spring and damping coefficients K_{11}, K_{22}, C_{11}, and C_{22} are determined from the STIRDYN dynamics code to achieve operation of the engine at the proper frequency (85 Hz) and displacer phase angle (70^o).
The damping coefficient connecting the piston to the alternator circuit, C_{32}, has the units Volt-second/meter (E-s/m, where E is the alternator generated voltage) and the corresponding coefficient connecting the alternator circuit to the piston, C_{23}, has the units Newton / ampere (F/A). Conservation of energy requires that the mechanical power delivered to the alternator by the piston (F*V) equals the mechanical power absorbed by the alternator (E*i), i.e.

$$-F \cdot v = E \cdot i \text{ ,or, } -\frac{F}{i} = \frac{E}{v}. \quad (1)$$

II. Model Equations

The differential equations describing the dynamics are given in equation (2).

$$m_{11}\ddot{x}_d + c_{11}\dot{x}_d + c_{12}\dot{x}_p + k_{11}x_d + k_{12}x_p = 0, \quad (2a)$$

$$m_{22}\ddot{x}_p + c_{21}\dot{x}_d + c_{22}\dot{x}_p + c_{23}\dot{q} + k_{21}x_d + k_{22}x_p = 0, \quad (2b)$$

$$m_{33}\ddot{q} + c_{32}\dot{x}_p + c_{33}\dot{q} + k_{33}q = v. \quad (2c)$$

If the temperature ratio of the engine was 1.0, then the k_{12} would be negative and equal to k_{21}. If the displacer rod area were zero and the temperature ratio of the engine was 0, then both spring terms would be zero. From the analysis the load resistance is estimated to be 31.053 Ω. Equation set (2) was used to develop a state space model (SSM) of the engine dynamics. The form of the SSM is given in equation (3).

$$[\dot{x}] = [A]x + [B]u \text{ and } [y] = [C]x \quad (3)$$

A, B and C are given as:

$$A = \begin{bmatrix} 0 & 1 & 0 & 0 & 0 & 0 \\ -k_{33}/m_{33} & -c_{33}/m_{33} & 0 & -c_{32}/m_{33} & 0 & 0 \\ 0 & 0 & 0 & 1 & 0 & 0 \\ 0 & -c_{23}/m_{22} & -k_{22}/m_{22} & -c_{22}/m_{22} & -k_{21}/m_{22} & -c_{21}/m_{22} \\ 0 & 0 & 0 & 0 & 0 & 1 \\ 0 & 0 & -k_{12}/m_{11} & -c_{12}/m_{11} & -k_{11}/m_{11} & -c_{11}/m_{11} \end{bmatrix},$$

$$A = \begin{bmatrix} 0 & 1 & 0 & 0 & 0 & 0 \\ -2.8524 & -.0006 & 0 & -.0154 & 0 & 0 \\ 0 & 0 & 0 & 1 & 0 & 0 \\ 0 & .0002 & -2.9787 & -.0002 & .4944 & .0001 \\ 0 & 0 & 0 & 0 & 0 & 1 \\ 0 & 0 & -.1563 & .0004 & -3.0113 & -.0005 \end{bmatrix} x10^5,$$

$$B = \begin{bmatrix} 0 \\ 1/m_{33} \\ 0 \\ 0 \\ 0 \\ 0 \end{bmatrix} = \begin{bmatrix} 0 \\ 14.042 \\ 0 \\ 0 \\ 0 \\ 0 \end{bmatrix}, \quad (4c)$$

$$C = \begin{bmatrix} 0 & 0 & 1 & 0 & 0 & 0 \end{bmatrix}. \quad (4d)$$

The state variables were selected as follows: x_1 =q (charge), x_2 = $\dot{q}$ (current), x_3 = x_p (piston displacement), x_4 = $\dot{x}_p$ (piston velocity), x_5 = x_d (displacer displacement), x_6 = $\dot{x}_d$ (displacer velocity). Note that the output voltage is a function of piston velocity and that c_{33} is the total resistance in series with the alternator. This includes the armature resistance and the load resistance. Also, c'_{33} (4.436 Ω) is the armature resistance. These coefficients for the linear model described in (4) are for the following operating conditions: head temperature (T_H) = 650°K, cold end temperature (T_C) = 325°K, piston stroke (x_P) = 11 mm, and c_{33} = 35.489 Ω.

III. Alternator Equivalent Circuit

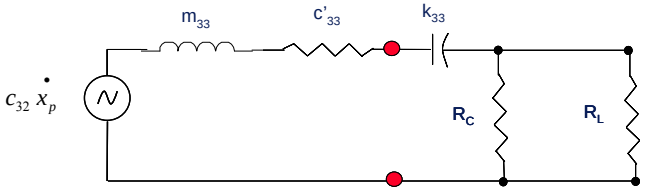

Figure 2: Electrical Equivalent Circuit

Figure 2 shows an equivalent electrical circuit for the FPSE alternator. The components are described as follows: R_C is the control resistance which is varied by the stroke controller output in order to maintain stroke setpoint. R_L is the load resistance. The alternator inductance is m_{33}. The tuning capacitance is k33 ($\omega \cdot m_{33} = 1/(\omega \cdot k_{33})$). The voltage proportionality constant is c_{32} (V·s/m). Notice that $c_{33} = c'_{33} + R_L \| R_C$. It is the value of c_{33} that determines the amplitude of the piston stroke.

IV. The Nonlinear Model

The nonlinearities are incorporated into the model using HFAST and STIRDYN to establish the relationships between the coefficients and the piston displacement. That is, $c_{jk} = f(x_p)$, $k_{jk} = f(x_p)$, and $m_{jk} = f(x_p)$. Since a 6th order model is used there are 36 coefficients to be established. After establishing all 36 coefficients for a number of piston stroke levels the nonlinear model was developed and programmed into Simulink® as shown in Figure 3.

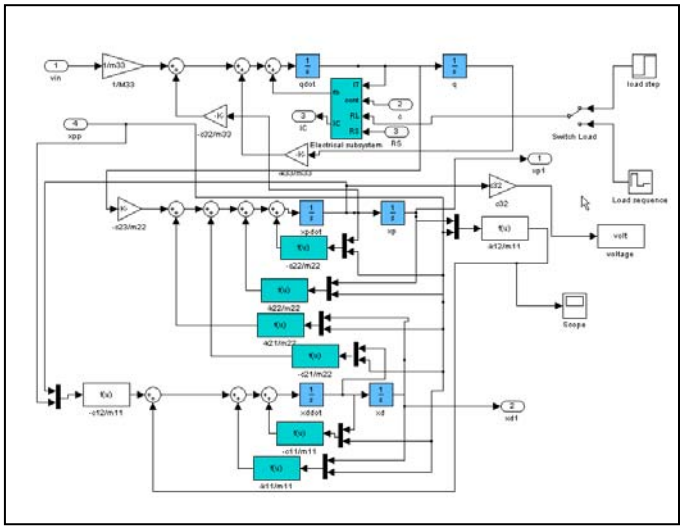

Figure 3: Nonlinear FPSE Model

V. The Open Loop Characteristics

There are two possible FPSE modes of operation. The first is stable and oscillatory and the other mode is stable but damped. With all other coefficients constant, c_{33} determines the mode of the dynamic system. If $c_{33} = 35.489$ Ω the system is stable and oscillatory. The eigenvalues (open loop poles) are located in the complex frequency plane as follows: -210.69±j486.34, -70±j563.12, 0±j534.07. The root locus and response are shown in Figure 4.

If c_{33} is decreased from 35.489 Ω to 23.996 Ω the stroke is reduced from 11 mm to 5 mm. The root locus for both values of c_{33} are shown if Figure 5.

The resistance change from 35.489 to 23.066 Ω has resulted in a significant change in the real parts of the complex conjugate pairs. This shows the sensitivity of these poles to changes in resistance. The poles closest to the imaginary axis will dominate the response as poles with large real parts result in a faster response and their affect on total response may be small compared to those close to the imaginary axis.
At some point reducing c_{33} will result the inability for the FPSE to maintain oscillation due to the internal magnetic forces and the engine will stall. The engine will stall when c_{33} <15 Ω.. Figure 6 represents the response to a load change with c_{33} changed from 40 to 14.3 Ω after ten seconds. In reality, c_{33} is changed by changing the value of R_L

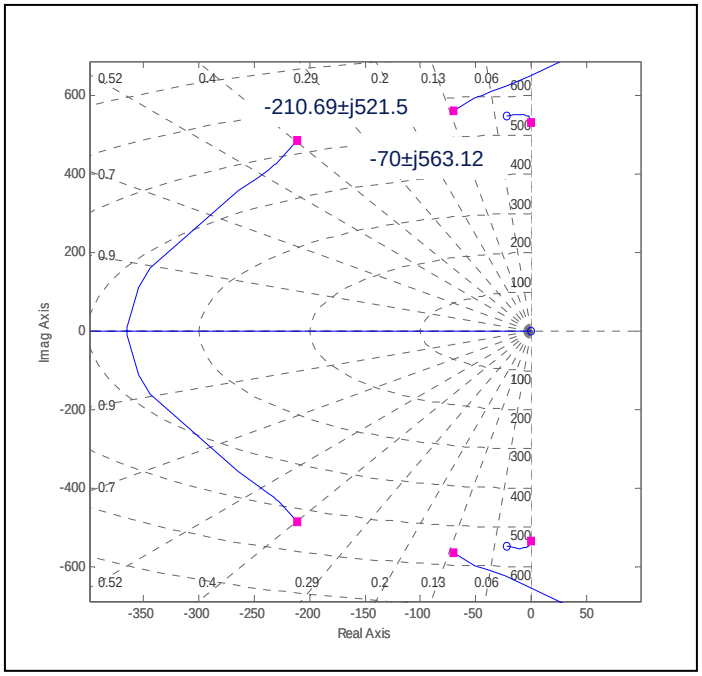

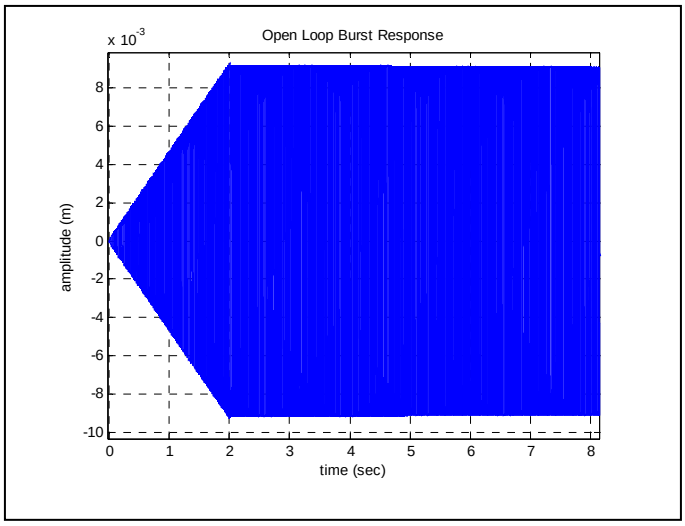

$x_P = 11$ mm , $T_H = 650°K$
$T_C = 325°K$, $c_{33} = 35.489$ Ω

Figure 4: Root Locus and Response with $c_{33} = 41.87$ Ω

Figures 5a and 5b show the root locus and pulse start response respectively for $c_{33} = 35.489$ Ω. Figure 5c and 5d

show the root locus and pulse start response respectively for c_{33} = 23.966 Ω.

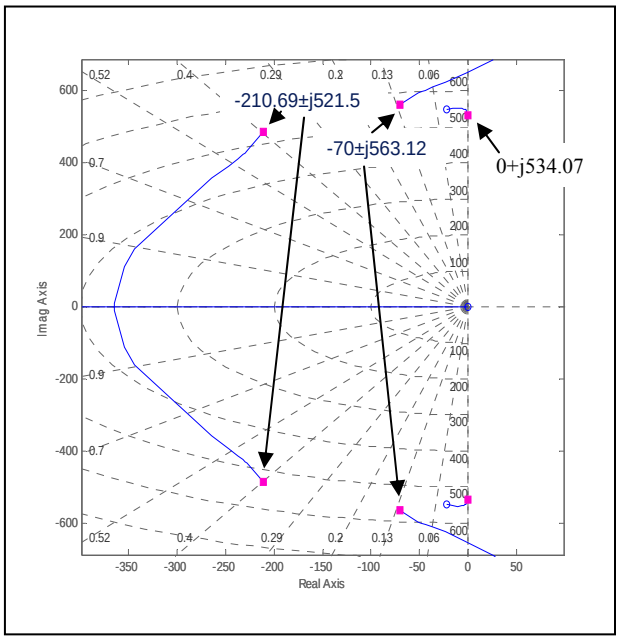

Figure 5a: Root Locus

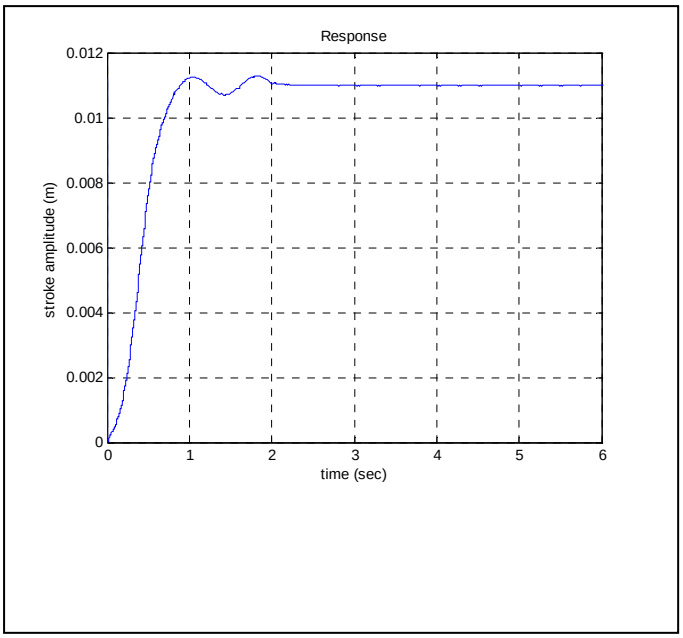

Figure 5b: Pulse Start Response

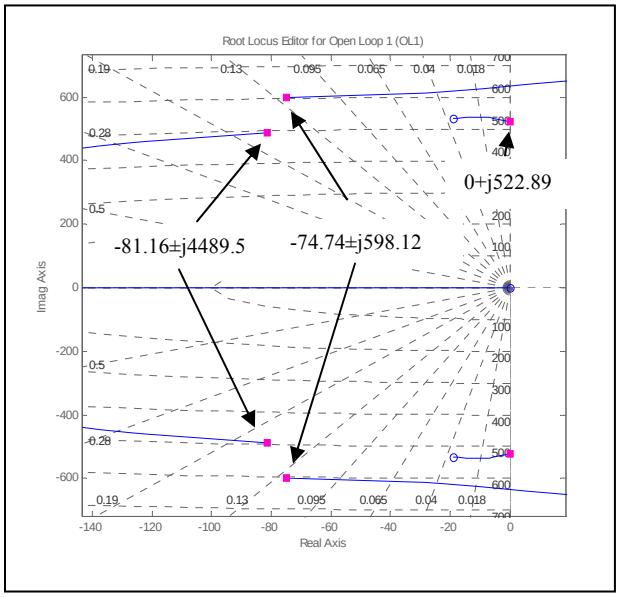

Figure 5c: Root Locus

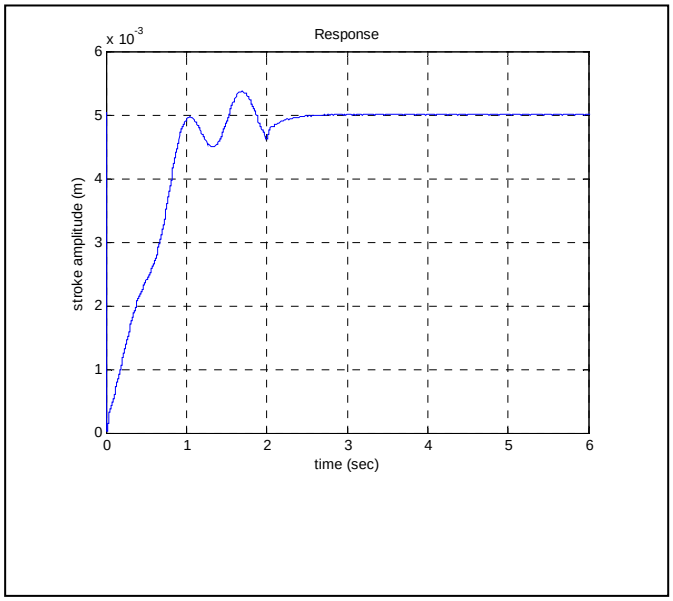

Figure 5d: Pulse Start Response

Figure 6 shows the effect of decreasing the load resistance to a point where the FPSE stalls. In this case a resistance value of 15 Ω will cause the FPSE to stall.

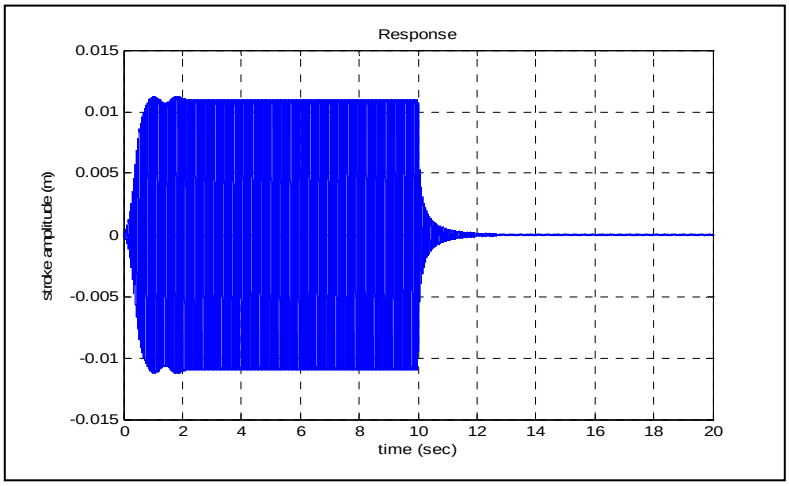

Figure 6: Response to Load Change

In order to establish the open loop dynamic characteristics of this engine a series of step response tests were conducted and a transfer function was established for each. Figure 7 shows the results of the step response tests. These tests were performed by changing R_L. Equation (5) shows the transfer function for four such tests.

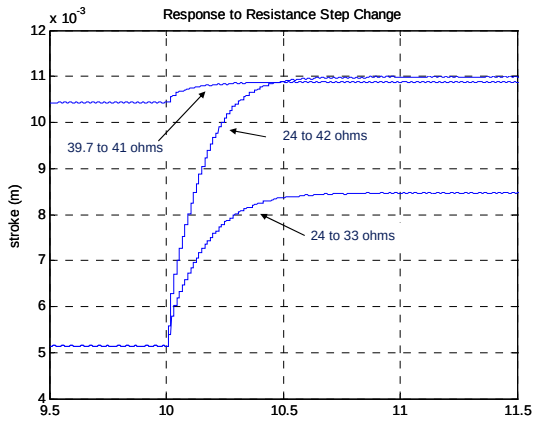

$$\frac{x_p(s)}{R(s)} = \frac{2.75\times10^{-3}}{s+7.14}, \text{24.4 to 33 ohm step}$$
$$\frac{x_p(s)}{R(s)} = \frac{2.57\times10^{-3}}{s+7.69}, \text{24.4 to 42 ohm step} \quad (5)$$
$$\frac{x_p(s)}{R(s)} = \frac{2.99\times10^{-3}}{s+10}, \text{33 to 38 ohm step}$$
$$\frac{x_p(s)}{R(s)} = \frac{3.8\times10^{-3}}{s+13.3}, \text{39.7 to 41.4 ohm step}$$

Figure 7: Load Step Response

Notice in (5) that the pole location and the gain change with each step change. This is due to the nonlinearity of the system. However, each response can be approximated with first order dynamics. This will be useful when tuning the controller as discussed in the next section. For example, if we constrain the stroke range between 5 and 11 mm we can use the first order dynamics described by the second transfer function in equation set (5).

VI. THE CONTROL STRATEGY

One method of holding the piston stroke at setpoint is to change c_{33} using a closed loop control system. A displacement transducer is used to measure the piston stroke and serve as the feedback, or process variable, in the closed loop control scheme. The output of the controller can change the total resistance via proportional pulse width modulation (PWM) switching of the control load. This keeps the stroke at the setpoint value. The duty cycle of the PWM signal will determine the effective value of R_C as shown in Figure 2.

The setpoint controller is an algorithm that adjusts the stroke setpoint to match the user load requirements. Therefore, a non-dissipative type control scheme is realized which essentially throttles the FPSE. A block diagram of the control scheme is shown in Figure 8. Control load current, user load current, and terminal voltage serve as inputs to the setpoint control algorithm. The output of the setpoint control algorithm is the stroke setpoint. The controller is capable of holding the piston stroke at the setpoint in the presence of both thermal and electrical load disturbances. However, the controller cannot cause the piston stroke to increase if the user load resistance R_L, which is in parallel with the control resistance R_C, is so small.

The controller also monitors the piston amplitude

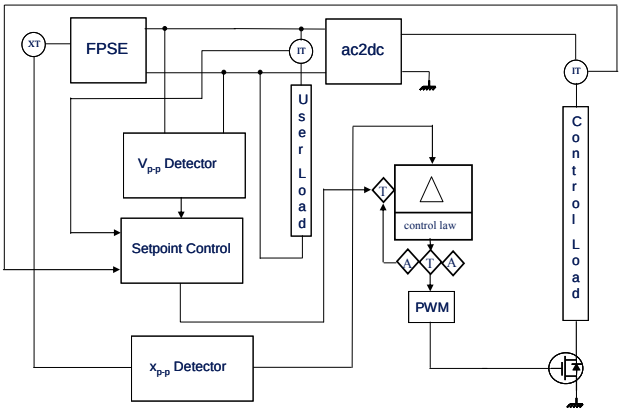

Figure 8: Control System Block Diagram

midpoint to ensure that if the midpoint drifts off center the

controller will reduce the setpoint to prevent the piston from hitting the mechanical limits. This is only possible if there is a piston stroke measurement in place. If voltage is used to control the stroke then this drift information is not present and over stroking could occur if the piston drifts off center. Since the output voltage is proportional to the piston velocity, the power output is reduced as the stroke amplitude is decreased. The controller should be able to respond to user load changes without significant overshoot which might result in the mechanical limits being reached.

From equation set (5) it is clear that the dynamics are not integrating processes. Therefore, integral action must be included in the control law to ensure that there is no offset error in the final stroke amplitude. Integral action places a pole at the origin and a zero on the real axis in the left plane. The placement of the zero determines the amount of integral. Placing this zero is part of the controller tuning.

The stroke setpoint is manipulated based on the user load demand. That is, as the user load is increased, load resistance is lowered, and the stroke setpoint is increased. As the user load is decreased the stroke setpoint is decreased. The result is a non-dissipative control which throttles the FPSE to match the user load. The control load current is minimized to conserve fuel.

VII. CONTROLLER TUNING

A proportional-Integral (PI) control law was incorporated in the controller. The PI control law transfer function is given by equation (6).

$$\frac{U(s)}{E(s)} = \frac{K_p(s + 1/\tau_I)}{s} = \frac{8.625(s + 7.69)}{s} \quad (6)$$

With the control law in place a series of closed loop load step changes were made. The FPSE was pulse started and after 10 seconds the load resistance was changed from 100 to 40 Ω. Then at 20 seconds the load resiatance was changed from 40 to 50 Ω. Finally, after 30 seconds the load resistance was changed from 50 to 100 Ω. The response plots are shown in Figure 9. Notice the response when the load resistance is changed from 40 to 50 Ω s.

The controller holds the stroke disturbance to about 9% when the load resistance is changed from 40 to 50 Ω. Increasing the integral gain (move the controler zero to the left) will further minimize the disturbance amplitude.

Figure 10 shows how the controller modulates the control resistance R_C to hold the piston stroke to a specific setpoint in response to a load disturbance. In Figure 10, R_L was changed from 40 to 50 Ω.

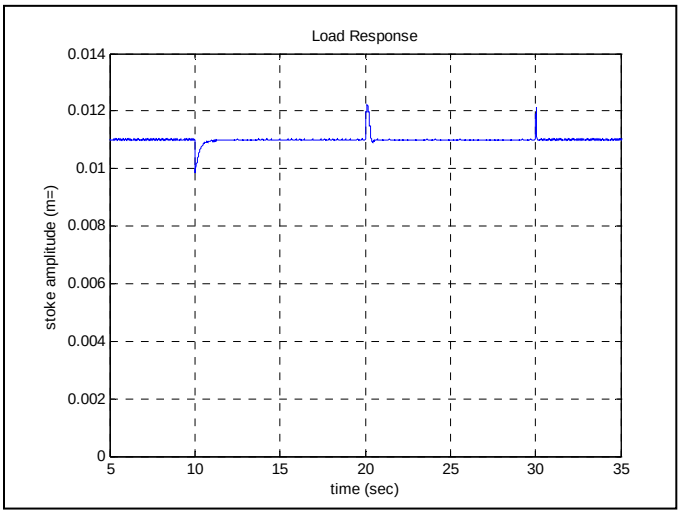

Figure 9: Load Disturbance Response

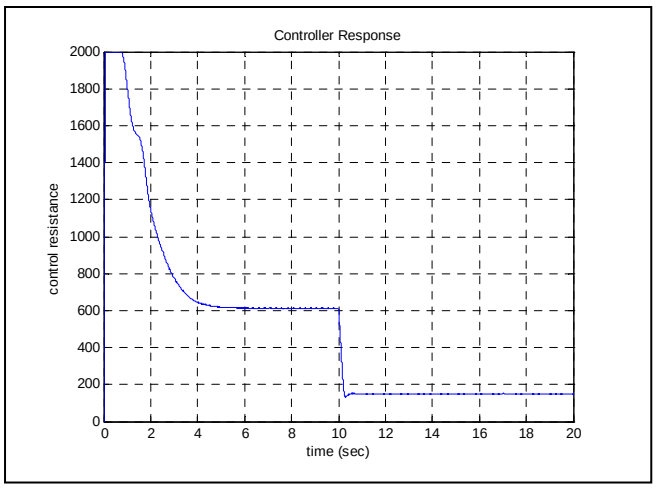

Figure 10: Controller Response

Figure 11 shows the response when a step change, from 0.0075 to 0.011 meters, is made in the stroke setpoint ten seconds after a pulse start.

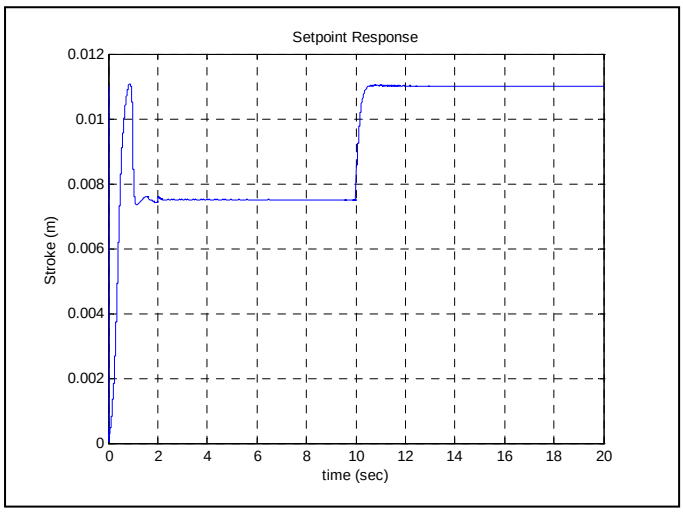

Figure 11: Setpoint Response

VIII. CONCLUSIONS

The dynamics of a FPSE can be modeled by a 6th order nonlinear model. It is possible to maintain stable operation of a FPSE, at a desired stroke amplitude setpoint, by modulating a control resistance in parallel with a user load. Since the 6th order model is a type 0 dynamic system, integral action is required to maintain an offset error of zero in the steady state.

From Figure 5 it is clear that the least dominant pair of complex poles are the most sensitive to load resistance. A 43% reduction in resistance engendered a 61% change in the real part of the least dominant poles but, only a 1.4% change in the most dominant pair.

The controller can be tuned based on a first order model of the transfer function between the stroke amplitude and the total resistance.

The work presented in this paper was based on a linear model of the FPSE that is currently being designed and built by Foster Miller, Inc. Once the engine is built the model and these results will be compared to the system. There are certainly a number of opportunities for nonlinearities to produce results that may differ form those obtained with this model. The nonlinearities can be identified and most of these can be incorporated into the model.

IX. ACKNOWLEDGMENTS

This work is supported by NASA through the Exploration Systems Mission Directorate for the Prometheus Program for the Fission Surface Power Project under NASA contract #NNC06CB81C "Development of High Efficiency, Free-Piston Stirling Converters." Any opinions expressed are those of the authors and do not reflect the views of NASA.

X. REFERENCES

[1] Regan, T.F., Gerber, S.S. and Roth, M.E., "Development of a Dynamic, End-to-End Free Piston Stirling Converter Model", in proceedings of the 37th Intersociety Energy Conversion Engineering Conference (IECEC 2002), 2002.

[2] Regan, T.F., Lewandowski, E.J., "Application of GRC Stirling Converter System Dynamic Model.", in the proceedings of the Second International Energy Conversion Engineering Conference (IECEC 2004) , AIAA, 2004.

[3] Benvenuto, G. and de Monte, F., "Electrodynamic Analysis of Free-Piston Stirling Engine/Linear Alternator Systems", August, 1994, published by the American Institute of Aeronautics and Astronautics, Washington, D.C., AIAA-94-4031-CP

[4] Kankam, M.D., Rauch, J, and Santiago, W., "Dynamic Analysis of Free-Piston Stirling Engine/Linear Alternator-

Load System-Experimentally Validated", National Aeronautics and Space Administration Report, NASA-TM-106034, 1992

[5] Huang: S. C. Huang, "HFAST – a harmonic analysis program for Stirling cycles," Proceedings of the 27th Intersociety Energy Conversion Engineering Conference, Vol. 5, 1992, pp. 47-52.).